Experimental Study of Turbidity Currents Flow around Obstacles

Riccardo Rossato and Elsa Alves

Laboratório Nacional de Engenharia Civil (LNEC)
Hydraulics and Environment Department
Av. Brasil, 101, 1700-066 Lisboa, Portugal
rrossato@lnec.pt; ealves@lnec.pt

Abstract

In artificial and natural reservoirs, turbidity currents can be an important mechanism for transporting fine sediments to the deepest area of the reservoir, where they settle. A solid obstacle can be placed at the bottom of the reservoir to partially block or divert the turbidity current flow preventing the deposition of sediments near intakes and other structures. A series of experiments were undertaken to investigate the influence of obstacles on turbidity currents flow dynamics, in particular, in the currents vertical velocity profiles and front velocity. Two series of laboratory tests with different obstacle heights were carried out in a channel 16.45 m long and 0.30 m wide with variable bottom slopes. To generate the turbidity currents a mixture of water and silica flour was used, considering different initial values of suspended sediments concentration. The results showed a reduction of the front velocity with the increasing obstacle height while the characteristic ratios of the velocity profiles remained constants.

1. Introduction

Sediment deposition in artificial or natural reservoirs can cause environmental, technical and economical problems. This natural process causes the loss of reservoir storage capacity and consequently the reduction of its long-term viability. Turbidity currents can play an important role in the deposition of fine sediments in reservoirs. These gravity currents are formed when the sediment-laden river enters into the lake and plunges beneath the clear water forming a dense underflow that moves downstream along the bottom of the reservoir. Their driving force is just gained from the suspended fine sediments that made the fluid heavier than the still water above it.

Over the last decades, advances have been made to characterize the turbidity currents flow (Parker et al., 1987; García, 1993; Altinakar et al., 1996; Hosseini et al., 2005; Alves, 2008; Sequeiros et al., 2010). These laboratory studies focused on the mean flow properties and on the vertical structure of the currents, namely, the shape of the velocity and suspended sediment concentration profiles, on the occurrence of hydraulic jumps and bed forms.

In recent years, some innovative techniques have been proposed to control and prevent turbidity currents sediment deposition in reservoirs. With the purpose of partially block or divert the turbidity current flows, the use of solid and permeable obstacles were studied by Oehy and Schleiss (2007) and the use of water jets by Oehy et al. (2010).

The influence of obstacles on gravity flows has also been studied in the past. Long (1970) considered the case of different velocities in the two layers fluids; Lane-Serff et al. (1995) studied the process considering three different types of upper flow. It was observed that the complete obstruction of the current occurs when the obstacle height is approximately twice the approaching gravity current height. Prinos (1999) worked with different obstacles geometries and found no important effects on the behaviour of the turbidity currents with the obstacle geometry. Oehy and Schleiss (2007) linked laboratory tests and 2-D numerical model results to study the velocity profiles and the sediment layer thickness with solid and

permeable obstacles. Leite Ribeiro et al. (2005) studied two technical solutions to manage the sedimentation in Livigno reservoir, respectively an underwater barrier close to the inlet and a permeable screen. Asghari Pari et al. (2010) investigated the effects of different obstacle heights on controlling the density currents produced by a saline solution.
Based on laboratory experiments, this paper examines the influence of the obstacle height on the hydrodynamics of plunging turbidity currents, namely, on the front velocity and on the average velocity profiles. The study represents an extension of the initial work by Rossato (2010).

2. Experimental Setup

2.1 Experimental Installation and Procedures

The experiments were carried out at the Hydraulics and Environment Department of Laboratório Nacional de Engenharia Civil (LNEC), in Lisbon. The channel is 16.45 m long, 0.30 m wide and 0.75 m maximum deep, with variable bottom slope. In Figure 1 a schematic view of the experimental setup is given. For a detailed description, the reader is referred to Alves (2008) and to Rossato (2010).

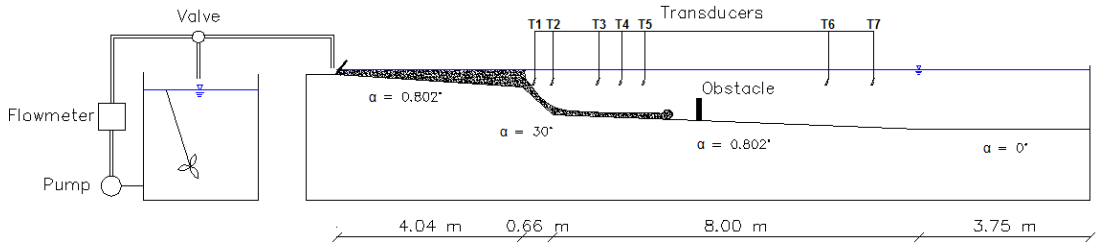

Figure 1: Experimental installation scheme

The configuration of the experimental installation allows the simulation of continuous plunging turbidity currents. The first 4.70 m long reach of the channel reproduce the entrance of a river in a reservoir where the deltaic deposition (coarse sediment deposits) occurs and the sediment-laden flow plunges to form a turbidity current. The downstream 11.75 m long reach is the reservoir in which the turbidity currents develops and flows over the obstacle.
The obstacles used in this study were made with Perspex with a rectangular shape 0.30 m wide and 0.009 m thickness. The experiments conducted with an obstacle 0.20 m high are designated by “Series A” and the experiments executed with an obstacle 0.25 m high by “Series B”. In both series, the obstacle was placed at 8.2 m from the entrance of the flume, 3.5 m after the deltaic slope. This position was defined to allow the complete development of the turbidity current, making possible to measure steady flow conditions before the current reached the obstacle and after the current passed the obstacle.
Before each experiment, the flume was filled with clear water. The mixture of water and sediment was supplied to the upstream end of the channel from a mixing tank with a capacity of 3.1 m^3. At the entrance of the flume, a diffuser reduced the flow velocity and allowed the distribution of the dense fluid across the entire channel width. At the end of the channel a drainage valve and an overfall weir assured a constant water level during the experiment.
The overall time of each experiment was approximately 11 minutes, during which several samples of water and sediment were taken close to the diffuser to characterize the initial volumetric concentration of the suspended sediments. The discharge of the water-sediment mixture was controlled by a valve and a calibrated electromagnetic flowmeter placed in the hydraulic circuit. Time measurements of the position of the front of the head of the turbidity current were taken with a chronometer.

Velocity profiles were measured with an Ultrasound Velocity Profiling (UVP) system by Met-Flow. Seven transducers were used; five were placed before the obstacle (at sections 4.3 m, 4.7 m, 5.7 m, 6.2 m and 6.7 m from the inlet of the channel) and two after the obstacle (at sections 10.7 m and 11.7 m from the inlet section).
The fine sediment used in the experiments was a silica flour with a density of 2650 kg/m^3 and a particle mean diameter D_{50}= 20 μm.

2.2 Experimental Parameters

Table 1 lists the initial conditions of the experiments, namely, Q_0 = inflow water-sediment discharge, C_{s0} = inflow suspended sediment concentration, ρ_w = density of the water inside the flume, ρ_m = density of the mixture and $g'_0 = g(\rho_m - \rho_w)/\rho_w$ = initial reduced gravity.

Table 1: Summary of the inflow conditions of the experiments

Test	Q_0 [l/s]	$C_{s\,0}$ [%]	ρ_w [kg/m^3]	ρ_m [kg/m^3]	g'_0 [m/s^2]	B_0 [cm^3/s^3]	Ri_0 [-]	Fr_{D0} [-]	Re [-]
A.01	0.70	0.444	998.34	1005.68	0.0721	168.2	0.62	1.27	1882
A.02	0.70	0.657	998.42	1009.27	0.1065	248.5	0.91	1.05	1882
A.03	0.70	0.232	998.50	1002.33	0.0376	87.8	0.32	1.76	1882
A.04	0.70	0.369	998.61	1004.70	0.0598	139.4	0.51	1.40	1882
A.05	0.70	0.795	998.78	1011.91	0.1289	300.7	1.10	0.95	1882
A.06	0.70	0.590	999.10	1008.85	0.0957	223.2	0.82	1.10	1882
A.07	0.70	0.317	998.95	1004.18	0.0514	120.0	0.44	1.51	1882
A.08	0.70	0.416	998.95	1005.81	0.0674	157.2	0.58	1.32	1882
A.09	0.70	0.790	999.01	1012.06	0.1281	298.8	1.10	0.95	1882
B.01	0.71	0.178	999.10	1002.04	0.0288	68.3	0.24	2.04	1909
B.02	0.71	0.337	999.10	1004.66	0.0546	129.2	0.45	1.48	1909
B.03	0.71	0.119	999.10	1001.06	0.0193	45.6	0.16	2.50	1909
B.05	0.73	0.232	999.10	1002.93	0.0376	91.5	0.30	1.84	1962
B.06	0.75	0.395	999.10	1005.62	0.0640	160.0	0.48	1.45	2016
B.07	0.69	0.530	999.10	1007.85	0.0859	197.5	0.76	1.15	1855
B.08	0.70	0.453	999.38	1006.86	0.0734	171.2	0.63	1.26	1882
B.09	0.70	0.316	999.38	1004.60	0.0512	119.4	0.44	1.51	1882
B.10	0.70	0.614	999.10	999.10	0.0995	232.1	0.85	1.08	1882

In the table, B_0 = buoyancy flux at the entrance of the flume, Ri_0 = initial Richardson number, Fr_{D0}= initial densimetric Froude number and Re = initial Reynolds number, defined by

$$B_0 = g'_0 q_0 \tag{1}$$

$$Ri_0 = \frac{1}{Fr_{D0}^{\,2}} = \frac{g'_0 h_0}{U_0^{\,2}} \tag{2}$$

$$Re = \frac{U_0 h_0}{\nu} \tag{3}$$

where q_0 = discharge per unit width and h_0, U_0 = initial height and velocity of the flow, respectively, and ν = kinematic viscosity of the fluid.
For the turbidity current flows presented here, Ri_0 is less than unity which corresponds to supercritical flows at the entrance of the reservoir, except in tests A.05 and A.09 where subcritical conditions are present. The Reynolds number is greater than 1000 in all the tests, ensuring turbulent flow conditions at the entrance of the reservoir.

3. Results and Discussion

3.1 Description of the Turbidity Current Flow over the Obstacle

A sequence of photographs showing the evolution of a typical turbidity current flowing over an obstacle is presented in Figure 2. When the turbidity current approached the obstacle (Figure 2a,b), the head of the current decelerated and climbed up (Figure 2c). Some of the dense fluid flowed over the obstacle while another part formed an internal bore that travelled upstream (Figure 2c,d,e) with a clear front. These bores moved up like a hydraulic jump (Figure 2e). Downstream the obstacle, the turbidity current is re-established and travelled along the flume with a head well defined (Figure 2f). After this first impact on the current, steady flow conditions were established downstream the obstacle and on the whole obstacle area until the end of the test. It should be noted that, in the experiments reported in this paper, the relation between the obstacle height and the average current height was less than two, which means that the turbidity current flow was not totally blocked and part of the current travelled over the obstacle.

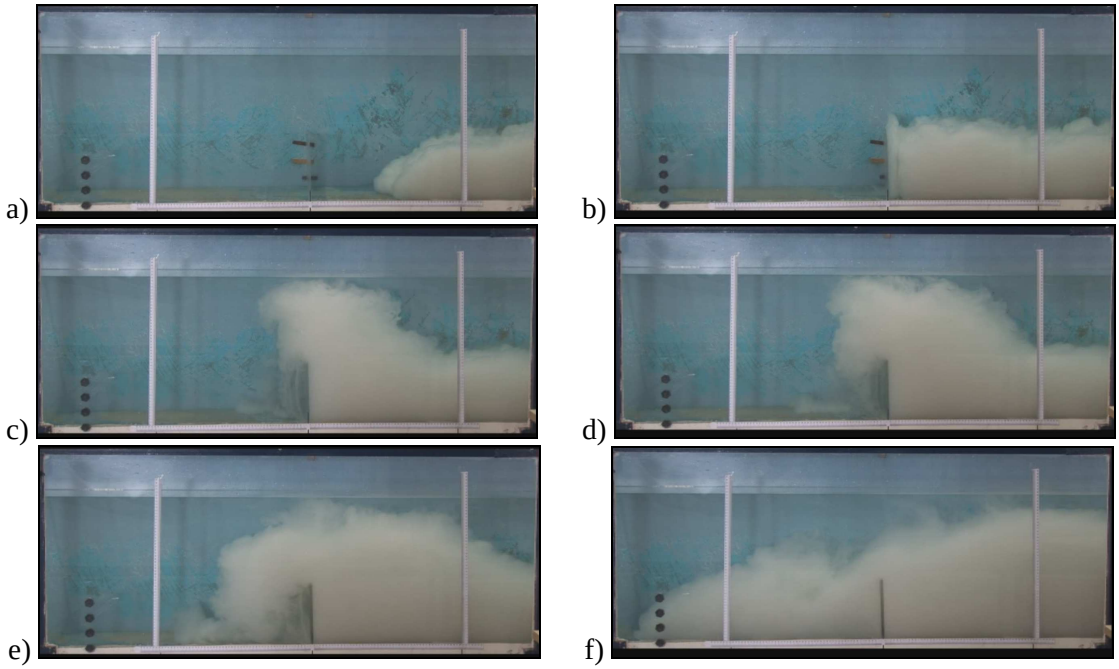

Figure 2: Photographic sequence of a turbidity current flowing over an obstacle

3.2 Front Velocity

In a previous laboratory study conducted in the same facility (Alves, 2008) with turbidity currents but without obstacles, it was concluded that the variation of the front velocity along the flume is small. Hence, it was assumed that the currents travelled with constant front velocity (U_{f1}). As observed by various authors the front velocity is related with the initial buoyancy flux by a constant relation given by the parameter l

$$l = U_{f1} / B_0^{1/3} \qquad (4)$$

Table 2 presents the average values of l obtained in this study considering the front velocity of the oncoming turbidity current upstream the obstacles. It can be seen that the values are in agreement with other studies.

Table 2: Average values of l obtained in different laboratory studies

Author	Type of current	Number of values	$U_{f1}/ B_0^{1/3}$
Altinakar (1988)	Turbidity current	47	0.91
Oehy (2002)	Turbidity current	9	1.01
Alves (2008)	Turbidity current	23	0.88
Present study	Turbidity current	17	0.88

In the present experiments, the obstacle effect on the front velocity of the turbidity current head can clearly be seen on Figure 3. In this figure, a comparison between values of the turbidity currents front velocity upstream (U_{f1}) and downstream (U_{f2}) the obstacle is presented for both series of experiments conducted with two obstacle heights. As expected, both obstacles induce a deceleration in the turbidity currents front. The decrease of front velocity is due to buoyancy flux loss as a result of the sediment deposition upstream the obstacle. The loss of sediments reduces the density difference between the current and the ambient fluid which is the driving force of head of the turbidity current.

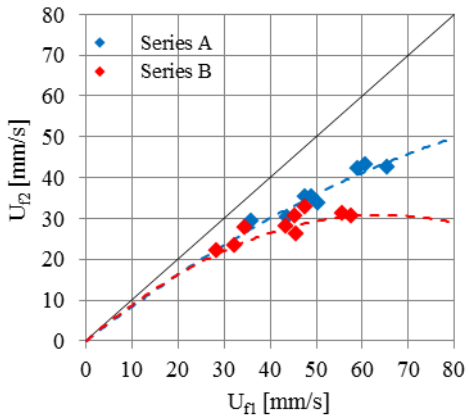

Figure 3: Relation between current front velocities upstream (U_{f1}) and downstream (U_{f2}) the obstacle

For similar values of front velocities of the approaching flow, the reduction of the head velocity is clearly higher in Series B (obstacle 0.25 m high) than in Series A (obstacle 0.20 m high). It also seems that the decrease of the front velocity is more accentuated with the increase of the oncoming head velocity. In the present experiments, downstream the obstacle the relation between the front velocity and the initial buoyancy flux ($U_{f2}/B_0^{1/3}$) decreases to 0.65 in Series A and to 0.56 in Series B, confirming the influence of the obstacle height.

3.3 Velocity Profiles

Figure 4 presents a typical velocity profile of the body of a continuous turbidity current flowing along the channel without the obstacle influence. Within the body of the current the velocity increases from zero at the bottom to a maximum value (U_{MAX}) at h_{MAX} and then decreases to zero at a distance h_t. The velocity profiles exhibit a reverse flow (return flow) produced by the shear stress at the interface between the current and the clear water. As observed in previous investigations (Altinakar et al., 1996; Alves et al., 2008) the velocity profiles of turbidity currents are similar to the ones of a wall jet: the wall region is defined between the bottom and the point of maximum velocity, and the jet region from this point to the position of the interface between the current and the ambient water. Experimentally, it was found that the relations h_{MAX}/h, U_{MAX}/U and h_t/h are almost constant.

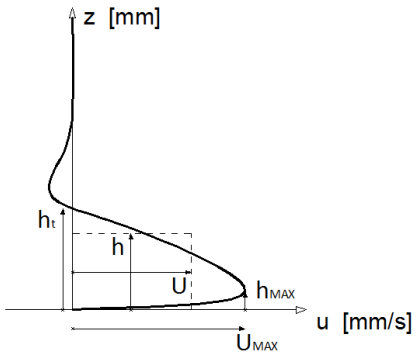

Figure 4: Typical velocity profile of a turbidity current

The average velocity (U) and height (h) of the currents body where obtained from the average velocity profiles, using the following moment equations:

$$Uh = \int_0^{h_t} u\,dz \tag{5}$$

$$U^2h = \int_0^{h_t} u^2 dz \tag{6}$$

where u = point velocity and z = vertical coordinate.

Although velocity profiles were measured in seven sections of the flume (see Figure 1), only the results of the transducers placed downstream the plunging region (T3 to T7) are considered here. Moreover, for the characterization of the approaching flow to the obstacle, the velocity profiles measured upstream the obstacle during the internal bore development were excluded. Figure 5 shows the dimensionless velocity profiles for A.02 and B.09 tests (obstacle heights 0.20 m and 0.25 m, respectively), obtained by the use of z/h and u/U.

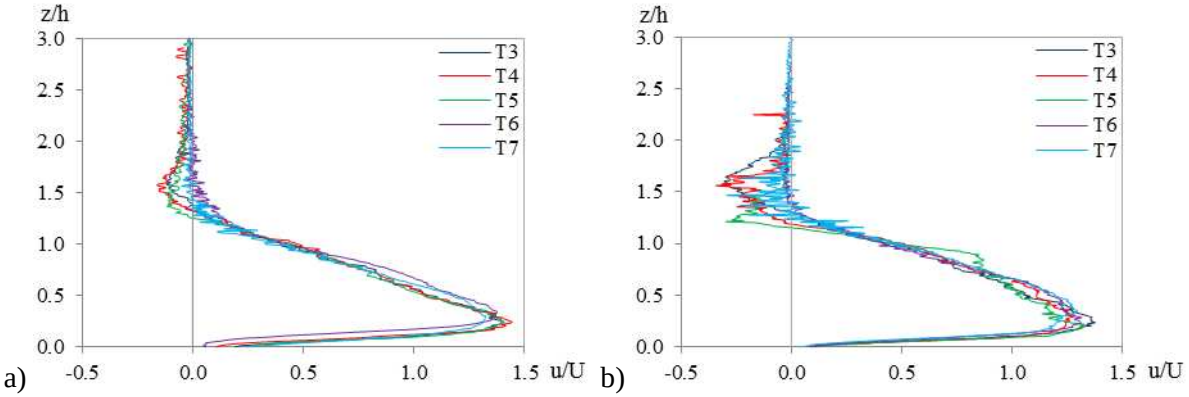

Figure 5: Dimensionless velocity profiles in A.02 and B.09 experiments

It is clearly seen that the velocity profiles collapsed into a single curve. It means that the structure of the velocity distribution does not change along the channel. Furthermore, the presence of the obstacle has no effects on the downstream velocity profiles of the turbidity currents (T6 and T7). Based on the velocity profiles, the average ratios h_{MAX}/h, U_{MAX}/U and h_t/h were calculated and summarized in Table 3, with the results of other laboratory studies of density currents. The results of this study are in good agreement with values of previous ones.

Table 3: Average values of h_{MAX}/h, U_{MAX}/U and h_t/h

Parameter	Altinakar (1988)	García (1993)	Altinakar et al. 1996)	Best et al. (2001)	Hosseini et al. (2005)	Alves (2008)	Sequeiros et al. (2010)	Present study
h_{MAX} / h	0.32	0.15 - 0.30	0.30	0.30		0.31	0.22 / 0.36 *	0.28
U_{MAX} / U			1.31		1.30	1.31	1.45 / 1.35 *	1.36
h_t / h			1.30		1.30	1.29	1.45 / 1.35 *	1.33

(*) The first values were obtained in experiments without bed forms and the second ones in experiments with bed forms

In Figure 6 average velocity profiles obtained in experiments with different obstacle heights but identical initial conditions are presented. For these comparisons two sections of the channel are considered: T4 at 6.2 m and T6 at 10.7 m from the channel entrance. These measurements allow the characterization of the velocity profiles of the oncoming flow and of the current downstream the obstacle. Although the obstacle height seems not to influence the relations h_{MAX}/h, U_{MAX}/U and h_t/h, the reduction of the maximum velocity (U_{MAX}) in T6 profiles is more accentuated for Series B tests. This is due to the higher retention of sediments upstream the obstacle in Series B that causes a loss of the density difference between the mixture and the clear water.

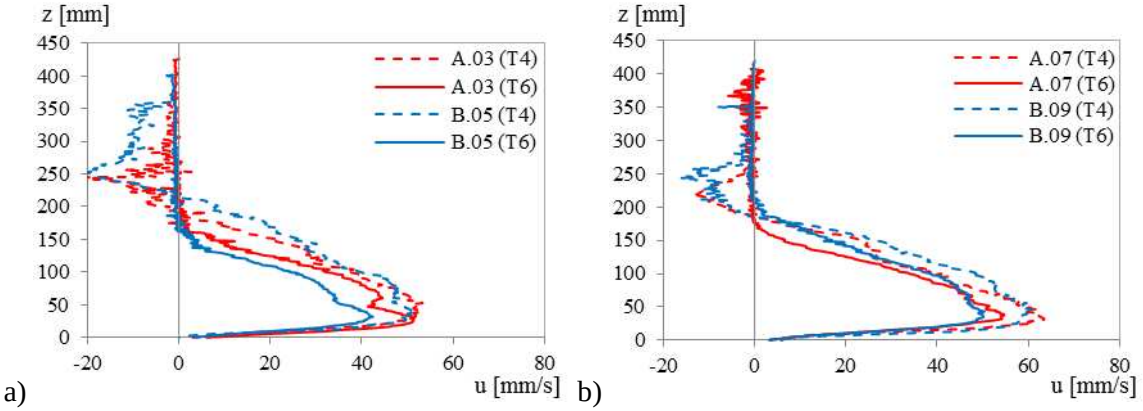

Figure 6: Comparison between velocity profiles upstream (dashed lines) and downstream the obstacle (solid lines) for experiments conducted with different obstacle heights and with similar initial conditions: a) A.03 and B.05 and b) A.07 and B.09

4. Conclusions

The influence of an obstacle height on turbidity currents front velocity and velocity profiles was experimentally investigated. The experiments were conducted with similar discharges varying the concentration of suspended sediments and the obstacle height. The front velocity of the turbidity current is noticeably reduced with the increase of the obstacle height, especially for higher values of the front velocity of the approaching current.

After the turbidity current passed the obstacle, the current flow is re-established and no significant influence of the obstacle was detected on the shape velocity profiles: the relations h_{MAX}/h, U_{MAX}/U and h_t/h kept constant along the channel. For similar inflow conditions, the reduction of the maximum velocity is more pronounced for the tests conducted with the higher obstacle.

Acknowledgments

The authors wish to acknowledge the financial support of the Portuguese Foundation for Science and Technology (FCT) through the research project PTDC/ECM/099485/2008. They also express gratitude to the technical staff of LNEC for the assistance on the laboratory work.

References

Altinakar, M. S. (1988). Weakly depositing turbidity currents on small slopes. *PhD Thesis*, Ecole Polytechnique Fédérale de Lausanne, Switzerland.

Altinakar, M. S.; Graf, W. H.; and Hopfinger, E. J. (1996). Flow structure in turbidity currents. *J. Hydraul. Res.*, 34:713-718.

Alves, E. (2008). Sedimentação em albufeiras por correntes de turbidez. *PhD Thesis*, Universidade Técnica de Lisboa, Instituto Superior Técnico, Portugal.

Alves, E., González, J., Freire, P., Cardoso, A. H. (2008). Experimental study of plunging turbidity currents in reservoirs. *River Flow 2008* – International Conference on Fluvial Hydraulics, Çesme-Izmir, Turquia, 3-5 September, 1157-1164.

Asghari Pari, S. A., Kashefipour, S. M., Ghomeshi, M., and Shafaie Bajestan, M. (2010). Effects of obstacle heights on controlling turbidity currents with different concentrations and discharges. *J. Food, Agric. & Envir.*, 8:930-935.

Best, J. L., Kirkbride, A. D., and Peakall, J. (2001). Mean flow and turbulence structure of sediment-laden gravity currents: new insights using ultrasonic Doppler velocity profiling. *Spec.Publs. int Ass. Sediment.*, 31:159-172.

García, M. H. (1993). Hydraulic jumps in sediment-driven bottom currents. *J. Hydraul. Eng.*, 119:1094-1117.

Hosseini, S. A., Shamsai, A., and Ataie-Ashtiani, B. (2005). Synchronous measurements of the velocity and concentration in low density turbidity currents using an Acoustic Doppler Velocimeter. *Flow Measur. and Instrum.*, 17:59-68.

Lane-Serff, G.F., Beal, L.M., and Hadfield, T. D. (1995). Gravity current flow over obstacles. *J. Fluid Mech.*, 292:39-53.

Leite Ribeiro, M., De Cesare, G., and Schleiss, A. J. (2005). Sedimentation management in the Livigno reservoir. *Hydropower and Dams*, 6:84-88.

Long, R. R. (1970). Blocking effects on flow over obstacles. *Tellus*, 22:471-480.

Oehy, C. D., and Schleiss, A. J. (2007). Control of turbidity currents in reservoirs by solid and permeable obstacles. *J. Hydraul. Eng.*, 133:637-648.

Oehy, C. D., De Cesare, G., and Schleiss, A. J. (2010). Effect of inclined jet screen on turbidity current. *J. Hydraul. Res.*, 48:81-90.

Parker, G., García, M., Fukushima, Y., and Yu, W. (1987). Experiments on turbidity current over an erodible bed. *J. Hydraul. Res.*, Vol. 25, pp. 123-147.

Prinos, P. (1999). Two-dimensional density currents over obstacles. *28th IAHR Congress*, Graz, Austria.

Rossato, R. (2010). Effect of obstacles on turbidity current hydrodynamics. *Master Thesis*, Università degli Studi di Padova, Italia.

Sequeiros, O. E., Spinewine, B., Beaubouef, R. T., Sun, T., García, M. H., and Parker, G. (2010). Characteristics of velocity and excess density profiles of saline underflows and turbidity currents flowing over a mobile bed. *J. Hydraul. Eng.*, 136:412-433.